INDOCHINA APPLIED SCIENCES

P. Phoempoon et al. / Indochin. Appl. Sci. 14(2) (2025) 260816

Research Article

The Effect of Silver Doping Concentrations in TiO_2 Nanoparticles: Characteristic, Morphological, Chemical, and Simple Regression Analyses

Phatcharee Phoempoon[a], Weerachai Sangchay[a,*], Kornkanok Ubolchollakhat[b], Kantamon Sukkrajang [a], Tanarat Rattanakool [a]

[a] *Faculty of Industrial Technology, Songkhla Rajabhat University, Songkhla, 90000, Thailand*
[b] *Faculty of Engineering, Thaksin University, Phatthalung Campus, Phatthalung, 93210, Thailand*

***Corresponding authors** *:* weerachai.sa@skru.ac.th
https://doi.org/10.55674/ias.v14i2.260816

Received: 14 February 2025; **Revised:** 23 April 2025; **Accepted:** 29 April 2025 ; **Available online:** 01 May 2025

Abstract

This research synthesizes silver-doped TiO_2 nanoparticles (TiO_2-Ag) using sol-gel and co-precipitation techniques, calcined at 500 °C for 1 h. Silver doping concentrations of 0, 1, 2, 4, 8, and 16 mol% in Titanium dioxide (TiO_2) were examined for their impact on particle size, shape, and phase. Characterization via EDX, XRD, TEM, and XPS. TEM micrographs show small, rounded particles (10 – 20 nm) forming clumps. Analyses revealed that increased silver content augments the rutile phase. Simple Regression Analysis was utilized to estimate phase quantity of the anatase and rutile phase of TiO_2-Ag.

Keywords*:* Titanium dioxide; Silver doping concentration; Sol-gel and precipitation methods; Morphological and chemical analyses; Simple regression analysis

1. Introduction

In the dynamic field of nanotechnology, the synthesis of advanced nanomaterials has become a cornerstone of scientific innovation, addressing critical challenges across environmental, energy, and medical domains. TiO_2 nanoparticles are renowned for their exceptional photocatalytic properties, chemical stability, and versatility. The particle size of TiO_2 nanoparticles plays a crucial role in determining their optical and electronic properties. As the particle size decreases to the nanometer scale, quantum size effects become significant. Specifically, when the particle size approaches or becomes smaller than the exciton Bohr radius, the band gap energy increases, leading to a blue shift in the absorption edge. This phenomenon allows for the tuning of TiO_2's optical properties, making it more suitable for applications such as photocatalysis and solar energy conversion. Therefore, controlling the nanoparticle size during synthesis is vital for optimizing their performance. However, the pursuit of enhancing these properties to meet the demands of modern applications has led researchers to explore various modifications. Among these, the doping of TiO_2 with silver (Ag) has emerged as a particularly promising strategy, leading to the development of TiO_2-Ag nanoparticles [1 – 3]. The synthesis of TiO_2-Ag nanoparticles is a sophisticated process that requires precise control over various parameters to achieve optimal properties. The incorporation of silver into the TiO_2 matrix significantly improves its photocatalytic efficiency, especially under visible light conditions. This enhancement is largely due to the unique plasmonic properties of silver, which facilitate increased light absorption and improved charge separation [4]. These attributes make TiO_2-Ag nanoparticles highly effective in a range of applications, including water purification, air quality improvement, and antimicrobial treatments. This introduction delves into the multifaceted process of synthesizing TiO_2-Ag nanoparticles, highlighting the methodologies, challenges, and innovations that define this area of research. Various synthesis techniques [5], such as sol-gel methods [6 – 9], hydrothermal processes [10], and chemical vapor deposition [11 – 12], offer different advantages and challenges. Each method must be meticulously tailored to control the size, shape, and distribution of silver within the TiO_2 nanoparticles, which are critical factors influencing their performance.

Characterization techniques play a crucial role in the synthesis process, providing insights into the structural, optical, and chemical properties of the nanoparticles. Methods such as X-ray diffraction (XRD), scanning electron microscopy (SEM), transmission electron microscopy (TEM), and ultraviolet-visible spectroscopy (UV-Vis) are employed to ensure that the nanoparticles meet the desired specifications and to understand the effects of silver doping on TiO_2. Band gap energy (Eg) values, estimated using Tauc plot analysis from UV-Vis absorption spectra, revealed that silver doping effectively reduced the band gap of TiO_2, enhancing its visible light photocatalytic activity. The band gap energy of pure anatase TiO_2 was approximately 3.20 eV, while silver-doped TiO_2 exhibited a narrowed band gap of 2.80 eV, indicating enhanced absorption in the visible spectrum [13]. Ag doping has been found to influence TiO_2 rutile-anatase phase transformation and favors grain growth [14]. There are several techniques available to estimate the crystallite size of a crystalline material, with the most commonly used being Transmittance Electron Microscope (TEM) and X-ray diffraction (XRD). TEM is more expensive and requires more maintenance and sample preparation compared to XRD. XRD is also commonly used for estimating crystallite size in crystalline materials. In addition to the Scherrer equation, there are other methods for calculating crystallite size including the Williamson-Hall plot, Monshi-Scherrer Model, Size-strain plot method, Halder-Wagner Model, and Sahadat-Scherrer Model. and Sahadat-Scherrer Model. All the models presented crystallite size in the accepted region, and Simple Regression Analysis coefficients were also taken into consideration [15 – 17]. In addition to the crystallite size, various intrinsic parameters such as stress, strain, energy density, and qualitative and quantitative phase analysis were also computed from the mentioned models based on XRD [15]. Titanium dioxide (TiO_2) exists in multiple crystalline forms, with anatase and rutile being the most commonly studied due to their unique and application-specific properties. Anatase is particularly valued for its high photocatalytic activity, which is useful in environmental purification, solar cells, and antibacterial surfaces. In contrast, rutile is more thermodynamically stable and is preferred in applications requiring thermal durability and optical performance, such as in pigments and coatings. Identifying and controlling the phase composition during synthesis is therefore crucial for tailoring TiO_2 materials toward desired applications.

This research aims to provide a comprehensive overview of the synthesis of TiO_2-Ag nanoparticles, exploring the various techniques, their underlying principles, and the innovations that have driven this field forward. By examining the synthesis process in detail, this study seeks to uncover new insights and strategies for optimizing the properties of TiO_2-Ag nanoparticles, thereby enhancing their applicability and effectiveness in solving real-world problems. The synthesis of TiO_2-Ag nanoparticles represents a significant advancement in the development of functional nanomaterials. This study involved synthesizing two phases of silver-doped TiO_2, Anatase and Rutile, using a straightforward procedure that only required the source of titanium, without the need for additional chemicals. Simple Regression Analysis based on X-ray diffraction was employed to predict the anatase-rutile phase form.

2. Materials and Methods

2.1 Synthesis of silver-doped TiO_2 nanoparticles

Prepare titanium (IV) isopropoxide volume 10 ml, dissolve in ethanol (C_2H_5OH, Merck, 99.50%) volume 100 ml, and dissolve silver nitrate ($AgNO_3$, VWR Prolabo, United Kingdom) volume 1, 2, 4, 8, 16 mol percent in Ethanol volume 50 ml. Adjust the pH with Sodium hydroxide at a concentration of 2 mol. It regulates the pH at about 6 to achieve a precipitation reaction. Dry the solution at 100 °C for 12 h. Calcined the synthetic powder at 500 °C for 1 h.

2.2 Characterizations

The Surface morphology and the size of TiO_2 nanoparticles were visualized using TEM (JEM-2010, JEOL). SEM with EDX spectrum was recorded with the help of Quanta FEG-250 to determine its homogeneity and its elemental distribution of elements in the investigated compound X-Ray Diffraction pattern of investigated TiO_2 nanoparticles was recorded by using (Phillips X'pert MPD, Cu-K). Structure of doping was determined by X-ray Photoelectron Spectroscopy (XPS, AXIS Ultra DLD, Kratos analytical Ltd.).

3. Results and Discussions

3.1 Characterization of TiO_2 and TiO_2 - Ag Nanoparticles

Synthesis of silver-doped titanium dioxide by sol-gel and precipitation methods revealed that the titanium dioxide sol was clear, while the silver-doped titanium dioxide sol appeared red, as shown in Fig. 1. Upon drying, as shown in Fig. 2, and calcination of pure TiO_2 and TiO_2-1Ag at 500 °C, the powders exhibited white and gray colors, respectively. The doping of these metals into titanium dioxide affected its color, as shown in Fig. 3. The TiO_2-1Ag powder changed color from white to gray after calcination due to the diffusion of silver from the bulk of titanium dioxide to the surface, resulting in silver doped into titanium dioxide in the form of Ag^0 and Ag_2O.

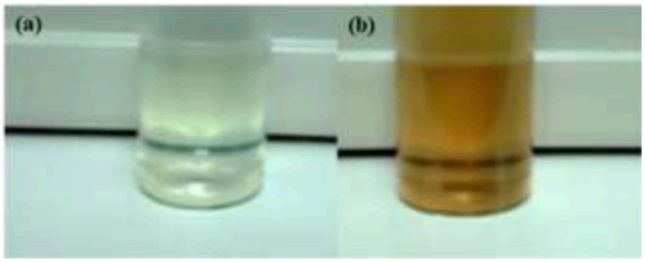

Fig. 1 Sol-Gel of (a) pure TiO_2 and (b) TiO_2 -1 Ag.

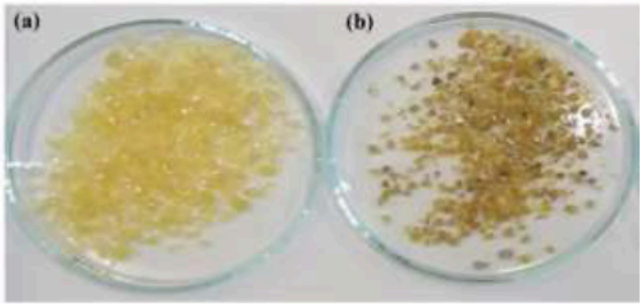

Fig. 2 Nanoparticles of (a) pure TiO_2 and (b) TiO_2 -1Ag before calcination.

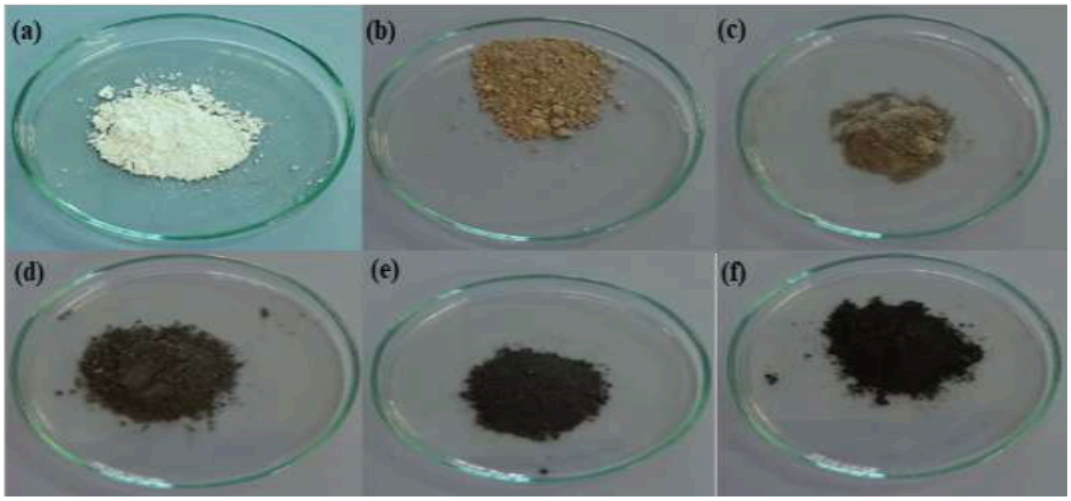

Fig. 3 TiO_2 powder calcined at 500°C for 1 h (a) pure TiO_2, (b) TiO_2-1Ag, (c) TiO_2-2Ag, (d) TiO_2-4Ag, (e) TiO_2-8Ag and (f) TiO_2-16Ag.

The identification of dopant elements in titanium dioxide, which confirms their presence, distribution, and bonding characteristics, can be performed using the EDX technique. As shown in Fig. 4, the TiO_2-16Ag powder was found to contain the elements titanium, silver, oxygen, carbon, and sodium.

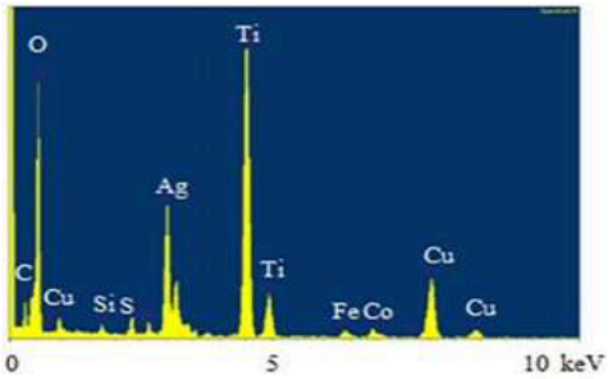

Fig. 4 Elemental analysis of TiO_2-16Ag nanoparticles after calcination at 500°C by using EDX technique.

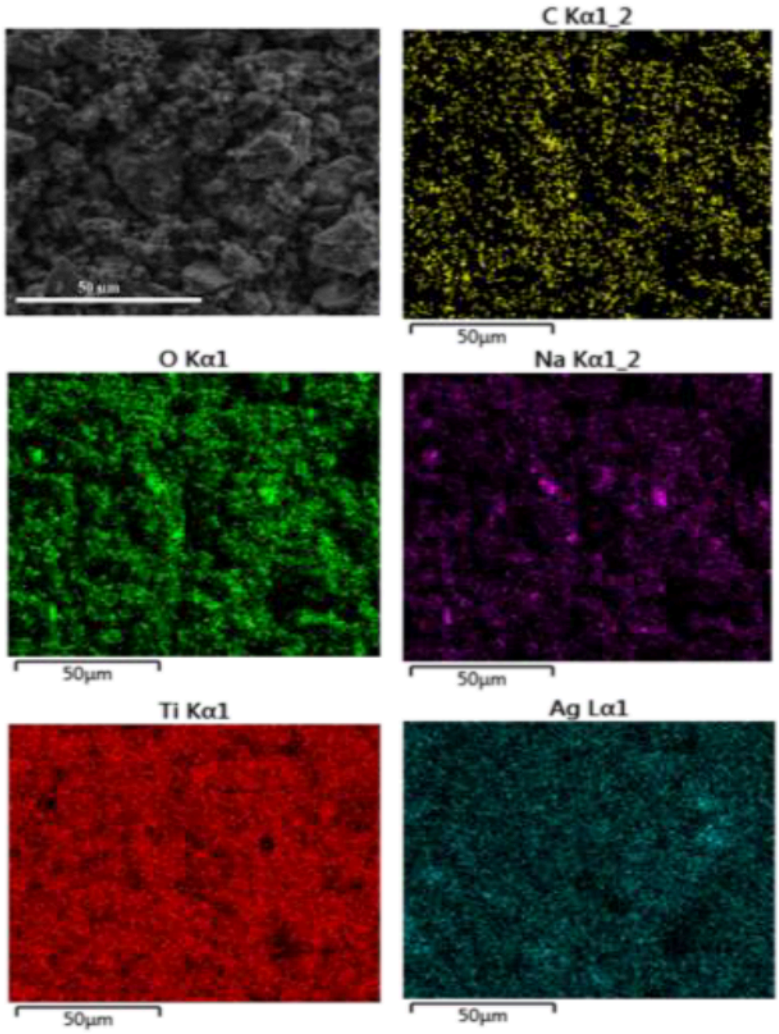

Fig. 5 Elemental composition analysis and distribution mapping of TiO_2-16Ag using EDX mapping techniques.

The presence of sodium is attributed to the use of NaOH in the pH adjustment and precipitation process. Additionally, the silver dopant was found to be well-distributed and uniform in the TiO_2, as shown in Fig. 5. It is important to note that trace signals of C, Si, S, Fe, Co, and Cu observed in the EDX spectrum are attributed to sample mounting materials, environmental exposure, and instrument-related background contamination. These elements were not introduced through the synthesis process and are commonly encountered in SEM/EDX analysis workflows. The EDX spectrum shows the presence of Na; however, the

elemental mapping does not indicate a significant distribution of Na across the sample area. This inconsistency may be due to localized contamination, instrumental sensitivity differences, or background interference. Since the mapping and spectra cover different areas and sensitivities, minor discrepancies in trace elements like Na are not uncommon and do not reflect the core composition of the TiO_2 nanoparticles.

The TEM image in Fig. 6 depicts the morphology and structure of the TiO_2-Ag nanoparticles synthesized using the sol-gel and co-precipitation technique, followed by heat treatment at 500 °C for 1 h. The TEM image in Fig. 6 presents a representative morphology of TiO_2-Ag nanoparticles synthesized at a selected silver concentration. Due to resource and equipment constraints, TEM imaging was performed only on this sample, which was chosen as a representative to reflect general particle size, shape, and aggregation behavior of the synthesized nanoparticles. The particles of the synthesized silver-doped TiO_2 nanoparticles exhibit a higher degree of agglomeration, forming clusters with a microscale size. The particles of TiO_2 powder appear to be in the range of approximately 10 – 20 nm. exhibiting a spherical morphology and aggregating together. The average crystallite size of TiO_2 and TiO_2-Ag nanoparticles was calculated using the Williamson-Hall (W-H) method based on the XRD data expressed in equation (1). The W-H equation accounts for both strain and crystallite size contributions to peak broadening:

$$\beta\cos\theta = \frac{k\lambda}{D} + 4\varepsilon\sin\theta \quad (1)$$

Where β is the full width at half maximum (FWHM) of the XRD peak (in radians), θ is the Bragg angle, k is the shape factor (typically 0.90), λ is the X-ray wavelength (0.15406 nm for Cu Kα), D is the crystallite size, and ε is the microstrain. The W-H plot was constructed by plotting $\beta\cos\theta$ versus $4\varepsilon\sin\theta$, and the crystallite size was extracted from the intercept. The resulting crystallite sizes ranged from X nm to Y nm, decreasing slightly with increasing Ag content due to lattice strain and dopant incorporation. TEM analysis confirmed the particle sizes to be in the range of 10 – 20 nm, consistent with the XRD results. The small difference between the two methods is attributed to the fact that XRD estimates the crystallite size (coherent scattering domain), while TEM provides the overall particle size, which may include agglomerates or multiple crystallites.

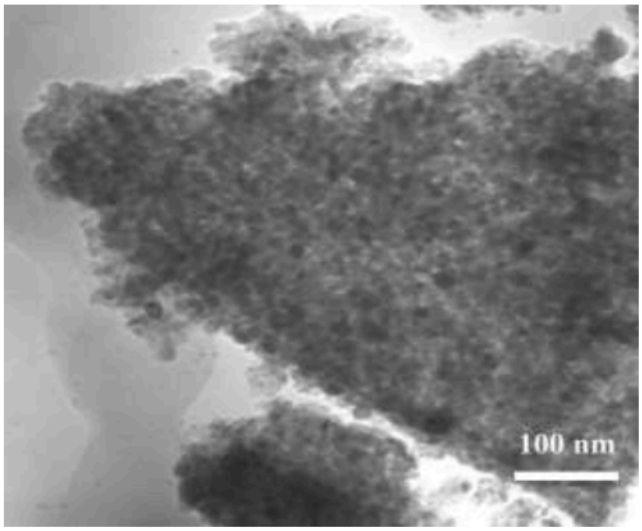

Fig. 6 TEM image of TiO_2-Ag nanoparticles synthesized via sol-gel and co-precipitation technique, calcined at 500 °C for 1 h.

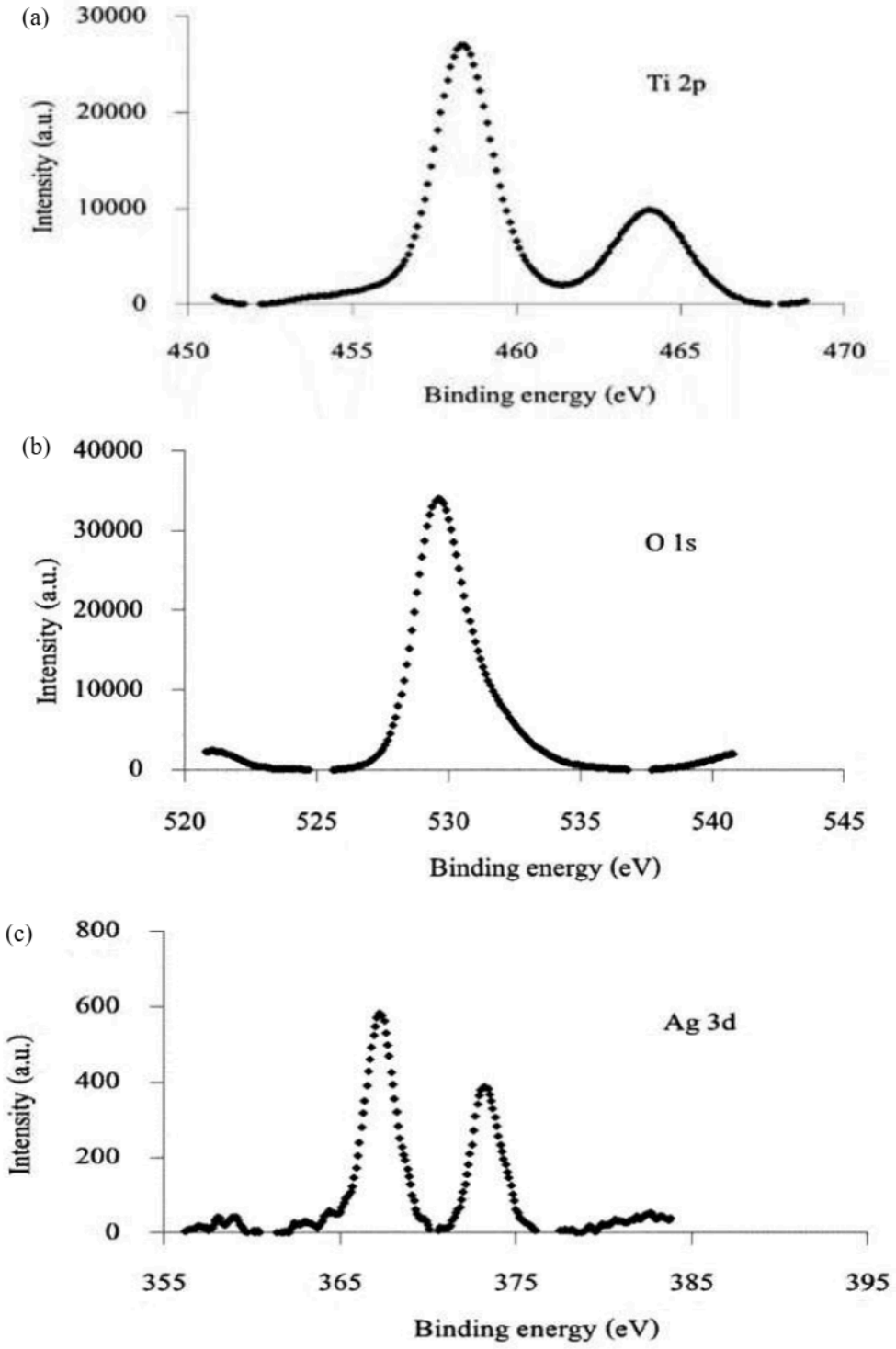

Fig. 7 The XPS spectra of TiO_2-1Ag nanoparticles.

The XPS analysis of the chemical structure reveals the presence of titanium, oxygen, and silver on the surface of the TiO_2-1Ag film. The binding energies of Ti $2p_{1/2}$ and $2p_{3/2}$ are observed at 464.10 and 458.40 eV, respectively. The O 1s peak appears at a binding energy of approximately 529.60 eV, while the binding energies of $Ag_{3/2}$ and $Ag_{5/2}$ are 367.20 and 373.20 eV, respectively. As depicted in Fig. 7, the chemical structure of the incorporated Ag in TiO_2 reveals a higher proportion of AgO

compared to Ag_2O. This is in accordance with the findings of H. Sutrisno et all. [18], who reported that the chemical structure of silver includes AgO, supported by $Ag_{3/2}$ at 367.30 eV, while the binding energy of Ag_2O is 367.80 eV. Additionally, the presence of Ag^+ is suggested by binding energies ranging from 368.04 – 368.13 eV, while the range of 366.28 to 366.58 eV indicates the presence of Ag^0.

Fig. 7 shows XPS spectra of TiO_2-Ag nanoparticles: (a) Ti 2p spectrum showing Ti^{4+} states at 464.10 eV and 458.40 eV, (b) O 1s spectrum indicating lattice oxygen at ~529.60 eV, and (c) Ag 3d spectrum showing peaks at 367.20 eV and 373.20 eV corresponding to Ag^{3+} species (mainly AgO). These results confirm the presence and chemical states of Ti, O, and Ag elements in the doped TiO_2 nanoparticles.

The X-ray diffraction (XRD) analysis of the TiO_2 and TiO_2-Ag nanoparticles (Fig. 8), subjected to a heating process at 500 °C for 1 h, exhibited well-defined diffraction patterns. TiO_2 and TiO_2-Ag nanoparticles powders showed a crystalline structure, comprising anatase and rutile phases. The characteristic peaks of anatase appeared at approximately 25.20°, 37.90°, 47.80°, 53.80°, and 55°, while the rutile phase was observed at around 27.40° (JCPDS 89-4921). The anatase phase displayed distinctive bending patterns at these positions, indicating the presence of anatase in the samples. Simultaneously, the rutile phase was identified at approximately 27.40° (JCPDS 89-4921). An increase in the quantity of silver led to the augmentation of the rutile phase, signifying the hindrance of the phase transition from anatase to rutile due to the presence of silver. The inhibition effect was more pronounced as the amount of silver increased. The diffraction pattern also revealed that the position of the silver particle peaks occurred around 38.1°, representing the primary position of silver particles (JCPDS 89-4921). The increase in the amount of added silver resulted in a more distinct peak at this position, indicating a clear presence of silver particles in the synthesized TiO_2-Ag nanoparticles. This supports the conclusion that the TiO_2-Ag nanoparticles, synthesized through the sol-gel and precipitation methods, The amount of anatase and rutile polymorphs in binary mixtures from XRD data as shown in Table 1.

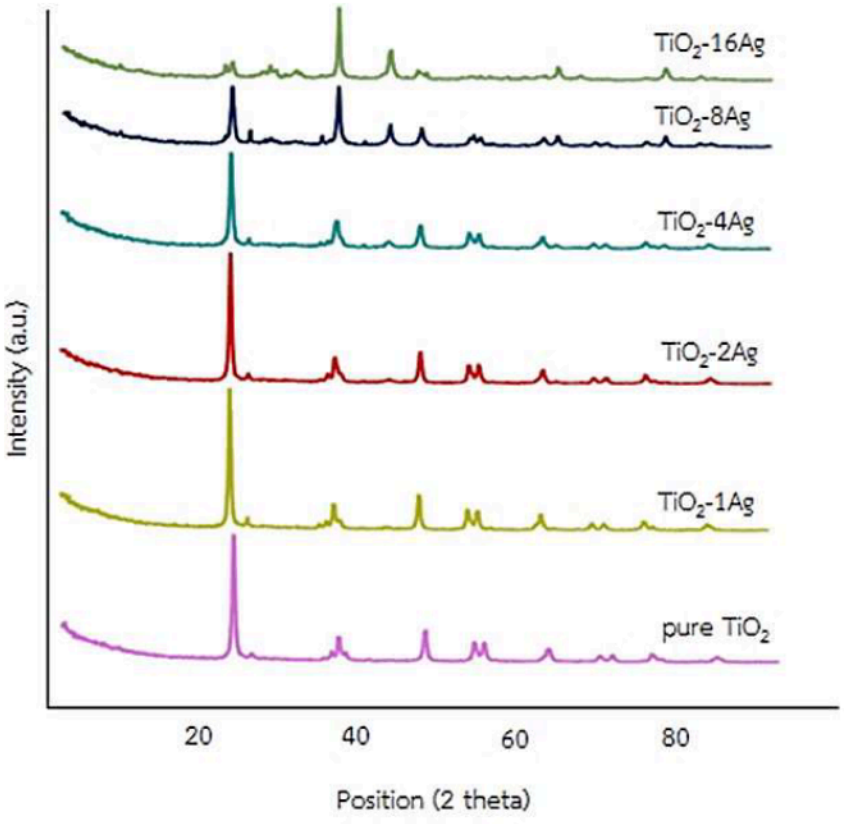

Fig. 8 The X-ray diffraction (XRD) analysis of pure TiO_2 and TiO_2-Ag nanoparticles.

Table 1 The amount of the anatase and rutile phases of TiO_2 and TiO_2-Ag.

Synthesized Substance	Phase Quantity (%)	
	Anatase Phase	Rutile Phase
pure TiO_2	97	3
TiO_2-1Ag	93	7
TiO_2-2Ag	95	5
TiO_2 4Ag	93	7
TiO_2-8Ag	80	20
TiO_2-16Ag	-	-

Table 2 Simple regression analysis results.

	β	Std. Error	Beta	T	p-value
Constant value (β_0)	97.525	1.812		53.824	.000
Silver content (β_1)	-1.975	.439	-.933	-4.494	.021*

For the amount of the anatase and rutile phases of TiO_2 and TiO_2-Ag were calculated using equations (1) and (2) [19].

$$W_a = k_aA_a/(k_aA_a+A_r) \quad (1)$$

$$W_r = A_r/(k_aA_a+A_r) \quad (2)$$

Where W_a and W_r represent the weight ratio of anatase and rutile phase. A_a and A_r are the peak intensity of anatase at the (101) plane and rutile at the (110) plane. k is the coefficient value as $k_a = 0.886$.

3.2 Simple Regression Analysis

Simple linear regression analysis is the analysis of a linear relationship between a primary variable (represented by x) and a dependent variable (represented by y), with only one primary variable having a linear relationship to each other. The data analysis aims to create a linear regression equation that best explains the relationship between the two variables. In this research, Simple linear regression was utilized to estimate the amount of anatase and rutile phase when various amounts of silver are doped to titanium dioxide. Basically, the simple linear regression model can be expressed as equation (3) [20].

$$y = \beta_0 + \beta_1x \quad (3)$$

In the simple linear regression model, y refers to the study or dependent variable as the amount of anatase phase, while x is the explanatory or independent variable as silver content. The expressions β_0 and β_1 are the parameters of the linear regression model. The β_0 parameter is regarded as an intercept term, while the β_1 parameter is regarded as the slope parameter. The general term for these parameters is known as regression coefficients. It also represents the variation between the observed and true realization of y. The results of the Simple Regression Analysis, which is calculated from a statistical program, are shown in Table 2.

Here, F = 20.197, R = .933, R^2 = .871, R^2_{adj} = .828, Std. Error = 2.778 and * P < .05 statistically significant at the level of .05. By replacing the value of β_1 (Silver content) in equation (3), the new equation can be expressed as equation (4)

$$y = 97.525 + (-1.975)x \quad (4)$$

From Table 2 and equation (4), it can be explained that the forecast equation can predict the coefficient of the data. The variability of the data value is predicted to be 87.10%, and when other factors are kept constant, an increase in the amount of silver will cause the phase to increase in the opposite direction.

Additionally, depending on the silver content, Simple Regression Analysis was used to forecast the anatase-rutile phase quantity [21]. A statistically significant result was obtained from the investigation, suggesting a high association between the relative quantities of rutile and anatase phases and silver doping. This work provides important new insights into the impact of silver doping on TiO_2 nanoparticles. According to the results, silver doping offers a viable way to adjust the phase composition of TiO_2 nanoparticles and maybe improve their photocatalytic and other characteristics.

4. Conclusion

This research successfully synthesized silver-doped TiO_2 nanoparticles using sol-gel and co-precipitation techniques followed by calcination at 500 °C for 1 h. The investigation of silver doping concentrations ranging from 0 – 16 mol% revealed its significant impact on particle size, shape, and phase transformation. Characterization techniques, including EDX, XRD, TEM, and XPS, provided insights into the materials' composition, morphology, and chemical structure. TEM micrographs illustrated the formation of small, rounded particles (10 – 20 nm) that exhibited a tendency to agglomerate into larger clusters. The XRD analysis confirmed the presence of both anatase and rutile phases in TiO_2 and TiO_2-Ag nanoparticles. Importantly, the study observed a clear trend of increased rutile phase content with increasing silver doping concentrations, suggesting that silver hinders the anatase-to-rutile phase transformation.

Acknowledgement

This research was supported by the Science Promotion Fund for Research and Innovation (NRCT) and Songkhla Rajabhat University. The researcher would like to express sincere gratitude to all individuals and organizations involved in this study. Special thanks are extended to the Faculty of Industrial Technology, Songkhla Rajabhat University, and the Faculty of Engineering, Thaksin University, for their support, facilitation, and coordination throughout the research process.

References

[1] Y. Suna, Y. Zhonga, X. Luoa, Y.J. Duana, K. Leia, L.J. Maoa, W. Fenga, Facile synthesis of N-doped TiO_2 nanosheets with exposed (001) facets for enhancing photocatalytic activity. Dig. J. Nanomater. Biostructures 18(4) (2023) 1147 – 1157.

[2] T. Munir, M. Sharif, H. Ali, M. Kashif, A. Sohail, N. Sabir, N. Amin, A. Mahmood, N. Ahmed, Impact of silver dopant on structural and optical properties of TiO_2 nanoparticles, Dig. J. Nanomater. Biostructures. 14(2) (2019) 279 – 284.

[3] K. Kotlhao, F.M. Mtunzi, V. Pakade, I.P. Ejidike, M.J. Klink, Synthesis, characterization and evaluation of Ag-TiO_2 nanocomposites for photo-catalytic degradation of selected chlorophenols, Dig. J. Nanomater. Biostructures. 13(3) (2018) 835 – 846.

[4] A. Modwia, B.R.Y. Abdulkhaira, M.E. Salih, N.Y. Elamina, A.M. Fatimaa, Fast and green synthesis of Sn/TiO_2 photocatalyst and it's bi-functional competence as adsorbent and photocatalyst, Dig. J. Nanomater. Biostructures. 14(2) (2019) 357 – 365.

[5] W.K. Abdulkadhim, Synthesis titanium dioxide nanoparticles doped with silver and novel antibacterial activity, J. Phys. Conf. Ser. 1999(1) (2021) 012033.

[6] S. Abbad, K. Guergouri, S. Gazaout, S. Djebabra, A. Zertal, R. Barille, M. Zaabat, Effect of silver doping on the photocatalytic activity of TiO_2 nanopowders synthesized by the sol-gel route, J. Environ. Chem. Eng. 8(3) (2020) 103718.

[7] M. Shabaninia, M. Khorasani, S. Baniyaghoob, Synthesis of Silver-Doped Titanium Dioxide Nanoparticles by Sol-Gel and Coprecipitation Techniques: Evaluation of Antimicrobial Activity and Cytotoxic Effects, ChemistrySelect. 9(1) (2024) 202303358.

[8] N. Yerli-Soylu, A. Akturk, Ö. Kabak, M. Erol-Taygun, F. Karbancioglu-Guler, S. Küçükbayrak, TiO_2 nanocomposite ceramics doped with silver nanoparticles for the photocatalytic degradation of methylene blue and antibacterial activity against Escherichia coli, Eng. Sci. Technol. Int J. 35 (2022) 101175.

[9] S.I. Mogal, V.G. Gandhi, M. Mishra, S. Tripathi, T. Shripathi, P.A. Joshi, D.O. Shah, Single-step synthesis of silver-doped titanium dioxide: influence of silver on structural, textural, and photocatalytic properties, Ind. Eng. Chem. Res. 53(14) (2014) 5749 – 5758.

[10] O. Avciata, Y. Benli, S. Gorduk, O. Koyun, Ag doped TiO_2 nanoparticles prepared by hydrothermal method and coating of the nanoparticles on the ceramic pellets for photocatalytic study: Surface properties and photoactivity, j. eng. technol. appl. sci. 1(1) (2016) 34 – 50.

[11] H. Chakhtouna, H. Benzeid, N. Zari, A. E.K. Qaiss, R. Bouhfid, Recent progress on Ag/TiO_2 photocatalysts: photocatalytic and bactericidal behaviors, Environ. Sci. Pollut. Res. 28(33) (2021) 44638 – 44666.

[12] K. Nagaraj, P. Thankamuniyandi, S. Kamalesu, S. Lokhandwala, N. M. Parekh, S. Sakthinathan, T.-W. Chiu, C. Karuppiah, Green synthesis, characterization and efficient photocatalytic study of hydrothermal-assisted Ag/TiO_2 nanocomposites, Inorg. Chem. Commun. 148 (2023) 110362.

[13] C. Bethel Anucha, I. Altin, E. Bacaksiz, I. Degirmencioglu, T. Kucukomeroglu, S. Yılmaz, V. N. Stathopoulos, Immobilized TiO_2/ZnO sensitized copper (II) phthalocyanine heterostructure for the degradation of ibuprofen under UV irradiation, Separations 8(3) (2021) 24.

[14] S. Rabhi, H. Belkacemi, M. Bououdina, A. Kerrami, L.A. Brahem, E. Sakher, Effect of Ag doping of TiO_2 nanoparticles on anatase-rutile phase transformation and excellent photodegradation of amlodipine besylate, Mater. Lett. 236 (2019) 640 – 643

[15] M.S. Hossain, S. Ahmed, Easy and green synthesis of TiO_2 (Anatase and Rutile): Estimation of crystallite size using Scherrer equation, Williamson-Hall plot, Monshi-Scherrer Model, size-strain plot, Halder-Wagner Model, Results in Materials 20 (2023) 100492.

[16] M.S. Hossain, M. Mahmud, M.B. Mobarak, S. Sultana, Md. A.A. Shaikh, S. Ahmed, New analytical models for precise calculation of crystallite size: application to synthetic hydroxyapatite and natural eggshell crystalline materials, Chem. Pap 76(11) (2022) 7245 – 7251.

[17] J. Madhavi, Comparison of average crystallite size by X-ray peak broadening and Williamson-Hall and size-strain plots for VO^{2+} doped ZnS/CdS composite nanopowder, Appl. Sci. 1(11) (2019) 1509.

[18] H. Sutrisno, A. Ariswan, D. Purwaningsih, Qualitative and quantitative phase-analysis of undoped titanium dioxide and chromium doped titanium dioxide from powder X-ray diffraction data, Indones. J. Chem. 18(3) (2018) 486.

[19] N. Altman, M. Krzywinski, Points of Significance: Simple linear regression, Nature Methods 12 (2015) 999 – 1000.

[20] F.G. Hartmann, J. Kopp, D. Lois, Social Science Data Analysis: An Introduction, Springer Fachmedien, Wiesbaden, 2023, pp.87 – 112.

[21] G. Madras, B.J. McCoy, A. Navrotsky, Kinetic Model for TiO_2 Polymorphic Transformation from Anatase to Rutile, J. Am. Ceram. Soc. 90(1) (2006) 250 – 255.